International Journal of Nanomedicine

Dovepress
open access to scientific and medical research

Open Access Full Text Article

ORIGINAL RESEARCH

Biomimetic component coating on 3D scaffolds using high bioactivity of mesoporous bioactive ceramics

International Journal of Nanomedicine downloaded from https://www.dovepress.com/
For personal use only.

This article was published in the following Dove Press journal:
International Journal of Nanomedicine
20 October 2011
Number of times this article has been viewed

Hui-suk Yun[1]
Sang-Hyun Kim[2]
Dongwoo Khang[3]
Jungil Choi[4]
Hui-hoon Kim[2]
Minji Kang[3]

[1]Functional Materials Division, Korea Institute of Materials Science, Gyeongnam, Korea; [2]Department of Pharmacology, School of Medicine, Kyungpook National University, Jung-Gu, Daegu, Korea; [3]School of Nano and Advanced Materials Science and Engineering and Center for NMBE, Gyeongsang National University, Jinju, Korea; [4]Department of Anatomy, Institute of Health Science and School of Medicine, Gyeongsang National University, Jinju, Gyeongnam, Korea

Background: Mesoporous bioactive glasses (MBGs) are very attractive materials for use in bone tissue regeneration because of their extraordinarily high bone-forming bioactivity in vitro. That is, MBGs may induce the rapid formation of hydroxy apatite (HA) in simulated body fluid (SBF), which is a major inorganic component of bone extracellular matrix (ECM) and comes with both good osteoconductivity and high affinity to adsorb proteins. Meanwhile, the high bioactivity of MBGs may lead to an abrupt initial local pH variation during the initial Ca ion-leaching from MBGs at the initial transplant stage, which may induce unexpected negative effects on using them in in vivo application. In this study we suggest a new way of using MBGs in bone tissue regeneration that can improve the strength and make up for the weakness of MBGs. We applied the outstanding bone-forming bioactivity of MBG to coat the main ECM components HA and collagen on the MBG-polycarplolactone (PCL) composite scaffolds for improving their function as bone scaffolds in tissue regeneration. This precoating process can also expect to reduce initial local pH variation of MBGs.

Methods and materials: The MBG-PCL scaffolds were immersed in the mixed solution of the collagen and SBF at 37°C for 24 hours. The coating of ECM components on the MBG-PCL scaffolds and the effect of ECM coating on in vitro cell behaviors were confirmed.

Results: The ECM components were fully coated on MBG-PCL scaffolds after immersing in SBF containing dilute collagen-I solution only for 24 hours due to the high bone-forming bioactivity of MBG. Both cell affinity and osteoconductivity of MBG-PCL scaffolds were dramatically enhanced by this precoating process.

Conclusion: The precoating process of ECM components on MBG-PCL scaffold using a high bioactivity of MBG was not only effective in enhancing the functionality of scaffolds but also effective in eliminating the unexpected side effect. The MBG-PCL scaffold-coated ECM components ideally satisfied the required conditions of scaffold in tissue engineering, including 3D well-interconnected pore structures with high porosity, good bioactivity, enhanced cell affinity, biocompatibility, osteoconductivity, and sufficient mechanical properties, and promise excellent potential application in the field of biomaterials.

Keywords: biomimic, mesoporous, ECM components, scaffold, bone regeneration

Introduction

Mesoporous materials synthesized via a sol-gel process and the supramolecular polymer templating methods are expected to have a range of applications in biomaterial science on account of their unique structural properties, including an ordered open pore structure ranging in size from 2 nm to 50 nm as well as a large specific surface area and pore volumes.[1–4] Bone tissue regeneration is the latest bioapplication using mesoporous materials.[5–21] The large specific surface area and pore volume of

Correspondence: Hui-suk Yun
Functional Materials Division, Korea Institute of Materials Science, 531 Changwondero, Changwon-Si, Gyeongnam 641-831, Korea
Tel +82 55 280 3351
Fax +82 55 280 3392
Email yuni@kims.re.kr

© 2011 Yun et al, publisher and licensee Dove Medical Press Ltd. This is an Open Access article which permits unrestricted noncommercial use, provided the original work is properly cited.

mesoporous materials dramatically enhance their bone-forming bioactive behavior and allow them to be loaded with osteogenic agents, thus promoting new bone formation, or with antibiotics for treatment purposes.[5,6] The development of mesoporous bioactive glasses (MBGs) has increased the use of mesoporous materials in tissue regeneration based on their superior hydroxy apatite (HA) deposition performance, ie, greater bone-forming bioactivity in vitro, when compared with normal sol-gel-derived BGs.[6] However, the meso-sized pores are too small to promote bone tissue regeneration. That is, MBGs are difficult to use alone as bone scaffolds for tissue regeneration at this stage.[10] The bone scaffold serves as a template for cell interactions and the formation of the bone extracellular matrix (ECM) for providing structural support to newly formed tissue.[22–25] An ideal scaffold, therefore, should have bone-mimicking features such as high porosity with a pore size between 10 μm and 1000 μm with a 3D interconnected pore structure, bioactivity, biodegradability, and biocompatibility. Sufficient mechanical strength and ease of processability are also required to match the intended site of implantation and handling. To compensate for the weak structural properties of MBGs and make them applicable for tissue regeneration, our group proposed and successfully prepared hierarchically 3D porous BG ceramic scaffolds using a combination of sol-gel, polymer templating, and rapid prototyping (RP) techniques, which can generate a physical model directly from computer-aided design data.[10] Even though these newly proposed BG scaffolds addressed the structural limitations of MBGs, their mechanical stability was lacking. For this, the development of a 3D porous MBG-polymer composite scaffold was constructed using the biodegradable polymer poly ε-caprolactone (PCL).[11] The MBG-PCL composite scaffolds possessed largely improved mechanical properties as well as molding capability, and they displayed effective in vitro bone-forming bioactivity. However, there still remain the problems to be solved not only relating to the high bioactivity of MBG accompanied with abrupt initial local pH variations, which may have unexpected negative effects such as cell damage when the scaffold is implanted in vivo, but also relating to the strong hydrophobicity of PCL, which may cause loss of cell recognition signaling.[26,27] To address these problems and improve the functionality of MBG as a bone scaffold, we applied the high bioactivity of MBG to coat biomimetic components on the surface of MBG-PCL scaffolds. That is, MBG may induce extraordinarily fast formation of HA on scaffolds in simulated body fluid (SBF), and we used this phenomenon to coat the main components of bone-ECM, HA, and collagen.

HA is a major inorganic component of bone ECM and has good osteoconductivity, high affinity to living cells, and the ability to adsorb proteins.[27–29] Meanwhile, the major organic component of bone ECM is collagen, which promotes early cell adhesion and interacts with osteoblasts.[28,30] The surface of the scaffolds plays an important role in interacting with host cells of tissue after implantation in situ.[31] Surface coating of MBG-PCL scaffolds combined with HA and collagen may provide for better interactions between scaffolds and cells compared with bare MBG-PCL scaffolds, resulting in improved tissue regeneration. Furthermore, the precoating process of ECM components on MBG-PCL scaffolds not only may improve the hydrophilicity of MBG-PCL scaffolds but also may eliminate initial variation in pH.

Materials and methods

Synthesis of MBG and preparation of gel paste for rapid prototyping

MBGs with 3D cubic pore structure were prepared according to our previously reported method.[32] In a typical synthesis, 2.88 g of F127 is dissolved in 18.1 mL of EtOH. Stock solutions, which were prepared by mixing 1.36 g of calcium nitrate tetrahydrate, 0.26 mL of triethyl phosphate, 6 mL of tetraethyl orthosilicate, 0.95 mL of HCl (1 M), 7.62 mL of ethyl alcohol, and 2.86 mL of H_2O, were added to this solution after stirring them for 1 hour separately and were vigorously stirred together for another 4 hours at 40°C. The reactant solution was transferred to a polystyrene vessel without a cap and aged at 40°C 40% RH for 48 hours without stirring. Gel films were obtained on evaporating the solvent. The obtained gel films were calcined at 600°C for 6 hours in air to remove the template. The MBGs were then ground and sieved. Granules with size below 25 μm were selected. PCL was dissolved in chloroform at 40°C, and the determined amounts of MBG powders (60 wt% of MBG to PCL) were then mixed with this to produce a homogeneous MBG-PCL paste. All chemicals were purchased from Sigma-Aldrich (St Louis, MO) and were used without further purification.

Fabrication of 3D scaffolds

The scaffolds were fabricated by directly extruding the gel paste onto a chilled substrate using a robotic deposition device.[11] A gantry robotic deposition apparatus was used with specially altered systems such as an actuator to control the position of the deposition nozzle for the fabrication of the scaffold and a heat-controlled blowing system to maintain the 3D scaffold morphology, followed by the rapid evaporation of the solvent. Three axes of motion control (x-, y-, and

z-axis) were provided by the gantry system, and a material delivery assembly composed of a syringe as a reservoir was affixed on the z-axis motion stage. The z-axis motion stage assembly was mounted on a moving gantry to enable the controlled motion of the mounted syringe in three dimensions. The gel paste housed in the syringe was deposited through a cylindrical nozzle (24 G [≈500 μm] is generally used). A linear actuator served to depress the plunger of the syringe at a fixed speed such that the volumetric flow rate could be precisely controlled. The extruding strength and speed were adjusted to 50 μL/minute and 10 mm/second, respectively. The shapes and sizes of the scaffold can be designed at discretion and can be controlled by a computer system.

Coating of ECM components

Collagen (type I [Col I]; Sigma-Aldrich, St Louis, MO) was dissolved in 0.1 M acetic acid (2 mg/mL). Two milliliters of this collagen solution was added to 200 mL of SBF. The SBF contained 142.0 mM Na^+, 5 mM K^+, 1.5 mM Mg^{2+}, 2.5 mM Ca^{2+}, 147.8 mM Cl^-, 4.2 mM HCO^{3-}, 1.0 mM HPO_4^{2-}, and 0.5 mM SO_4^{2-}.[33] Its chemical composition was similar to that of human plasma. The solution had a pH of 7.4 and was kept at 37°C before use. The MBG-PCL scaffolds were immersed in the mixed solution of the collagen-SBF at 37°C for 24 hours. After soaking, each scaffold was collected from the SBF, rinsed, and air dried.

Characterization

Characterization of structure and cell morphology was carried out by field emission scanning electron microscopy (FE-SEM) (Hitachi-S5500; Hitachi, Tokyo, Japan and JEOL-5800, Tokyo, Japan). Cell morphology was also studied using a fluorescence microscope (BX51; Olympus, Tokyo, Japan) with Meta Morph software (Olympus) after incubating for 6 hours at a density of 3×10^4 cells/well. The compressive modulus was determined using a micro load system (R&B Inc, Daejeon, Korea) at a head speed of 0.5 mm/minute. The porosity was measured by the Hg intrusion method (AutoPore IV 9510; Micromeritics, Norcross, GA). Wettability was observed using the contact angle measurement system (Phoenix-300, Surface Electro Optics, Gyunggido, Korea) after dropping 10 μL of water onto each scaffold. X-ray photoelectron spectroscopy (XPS) (ESCALAB 250; Thermo Scientific, Waltham, MA) was used to study the scaffold surface with ALKα electron source. Protein concentration was measured using a protein assay kit (Coomassie Plus 23236; Thermo Scientific). The absorbance at 595 nm was read using a spectrophotometer (Asys UVM 340; Biochrom, Holliston, MA).

Cell culture

Cell culture experiments were performed using a mouse calvaria-derived preosteoblast MC3T3-E1 subclone 4 cell line obtained from American Type Cell Culture Collection (ATCC, Manassas, VA). Cells were maintained in α-minimum essential medium (Gibco BRL Life Technologies, Grand Island, NY) containing 10% fetal bovine serum (Gibco BRL Life Technologies), 100 U/mL penicillin (Keunhwa Pharmaceutical, Seoul, Korea), and 100 U/mL streptomycin (Donga Pharmaceutical, Seoul, Korea). The cells were cultured under 100% humidity and 5% CO_2 at 37°C. The medium was changed every other day and, prior to confluence, cells were passaged using 0.05% trypsin/0.02% EDTA.

Initial cell attachment and cell proliferation

Cell attachment and proliferation were evaluated by a colorimetric assay based on the conversion of a 3-(4,5-dimethylthiazol-2-yl)-2,5-diphenyltetrazolium bromide (MTT, Sigma-Aldrich). MC3T3-E1 was seeded onto a square-shaped scaffold at a density of 1×10^5 cells/mL and cultured for 3 hours, 1 day, 3 days, 5 days, and 7 days. Each scaffold was prewetted in culture medium for at least 3 hours and then placed in a well plate.

Alkaline phosphate activity

Total cellular alkaline phosphate (ALP) activity of the cell lysates was measured in 2-amino-2-methyl-1-propanol buffer, pH 10.3, at 37°C using *p*-nitrophenyl phosphate as the substrate. The absorbance change at 405 nm was measured using a microplate reader. ALP activity was expressed as nanomoles of *p*-nitrophenol liberated per microgram of total cellular protein.

Quantitative real-time polymerase chain reaction

Quantitative real-time polymerase chain reaction (PCR) was carried out using the Thermal Cycler Dice TP850 (Takarabio Inc, Shiga, Japan) according to the manufacturer's protocol. Briefly, 2 μL of cDNA (100 ng), sense and antisense primer solution (1 μL, 0.4 μM), SYBR Premix Ex Taq (12.5 μL, Takarabio Inc), and dH_2O (9.5 μL) were mixed together to obtain a final reaction mixture (25 μL) in each reaction tube. Quantitative real-time PCR was carried out with the following primers: RUNX2 (s 5′-TAA GAA GAG CCA GGC AGG TG-3′; as 5′-TGG CAG GTA CGT GTG GTA GT-3′), Col 1 (s 5′-ATC CAA CGA GAT CGA GCT CA-3′; as 5′-GGC CAA TGT CTA GTC CGA AT-3′), ALP (s 5′-CTT GAC TGT GGT TAC TGC TG-3′; as 5′-GAG CGT AAT CTA CCA TGG

AG-3′), OP (s 5′-TCA AGT CAG CTG GAT GAA CC-3′; as 5′-CTT GTC CTT GTG GCT GTG AA-3′), and OC (s 5′-TGC TTG TGA CGA GCT ATC AG-3′; as 5′-GTG ACA TCC ATA CTT GCA GG-3′). β-actin (s 5′-tag-3′; as 5′-TGG CAG GTA CGT GTG GTA GT-3′) was used to verify equal amounts of cDNA. The amplification conditions were 10 seconds at 95°C, 40 cycles of 5 seconds at 95°C and 30 seconds at 60°C, 15 seconds at 95°C, 30 seconds at 60°C, and 15 seconds at 95°C. Relative quantification of mRNA expression was performed using the TP850 software.

Statistical analysis

The results were expressed as mean ± standard deviation. Statistical analyses were performed using GraphPad Prism (GraphPad Software Institute, San Diego, CA). Treatment effects were analyzed using one-way analysis of variance. Significance was set at $P < 0.05$.

Results and discussion

Coating of ECM components on MBG-PCL scaffolds

The synthetic strategy is illustrated in Scheme 1. We preliminarily prepared 3D MBG-PCL scaffolds according to our previously reported method.[11] The pore size and the porosity of MBG-PCL scaffolds was about 500 μm and 70%, respectively, with well-interconnected pores in three dimensions. The scaffolds were immersed in SBF containing dilute Col I solution at 37°C for 24 hours to form HA/collagen composite coatings on the scaffolds using high bioactivity of MBG (designated by ECM-coated scaffold). The abrupt initial local pH variations occurred during this stage because of initial release of Ca ions from the MBG. MBGs facilitate the rapid and massive release of Ca ions and subsequently induce high bioactivity.[6] Both Ca and P ions play an important role in promoting the formation of an extracellular mineralized matrix.[34] However, this property may also induce serious negative effects such as an inflammatory response, due to the sudden change of the pH value.[18,29,35,36] The abrupt initial pH variations were largely reduced during the biomimetic coating process and may reduce negative effects from the abrupt pH variation in vivo. The pH value of the solution for ECM-coated scaffolds after 1 day of immersion was around 8, whereas the pH value for MBG-PCL scaffolds was around 9.8 (Figure 1A).

The surface morphology of the MBG-PCL scaffolds started to change after treatment with SBF/collagen solution for 4 hours (see Figure S1). The MBG-PCL scaffolds immersed in SBF/collagen solution for 24 hours exhibited a rough surface morphology with fully covered HA-like particles and collagen fibers (Figure 2C and 2D, and Figure S2), whereas uncoated MBG-PCL scaffolds had a smooth surface morphology (Figure 2A and B). The formation of HA and collagen composites on the surface of the scaffolds was also confirmed by XPS, as shown in Figure 1B. Only weak Ca (345 eV) and Si (152 eV) peaks were detected from MBG-PCL scaffolds, proving the nonexistence of HA before the coating process. The weak peaks suggest that many parts of MBG were masked

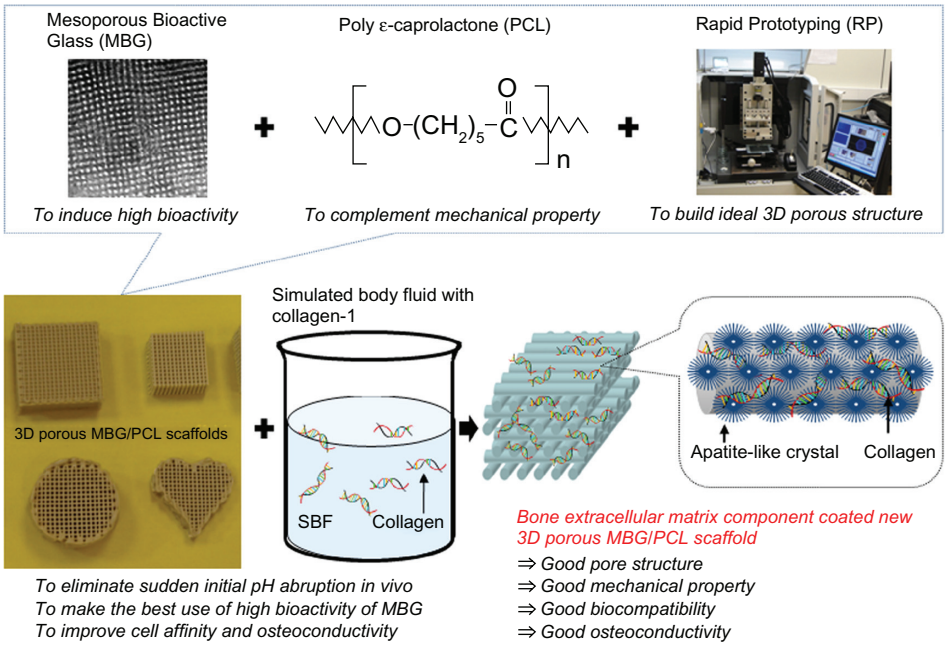

Scheme 1 Processing routes of extracellular matrix component-coated MBG/PCL scaffolds.

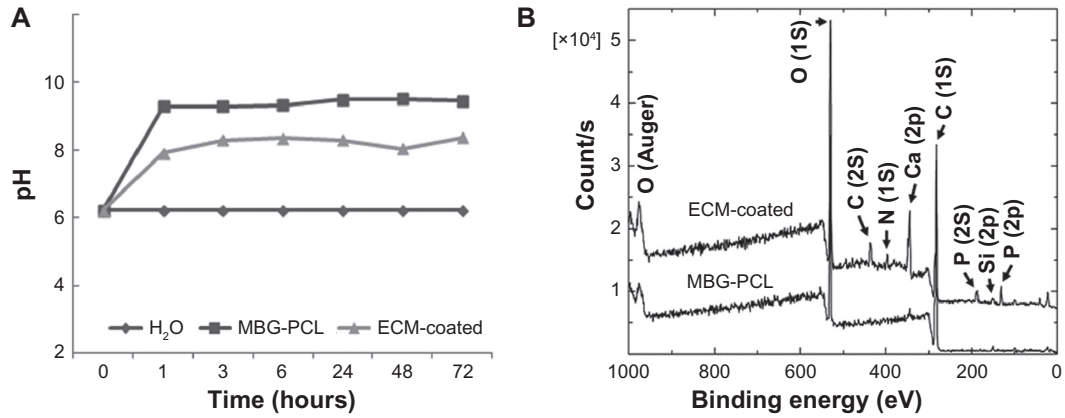

Figure 1 Comparison of pH variation of mesoporous bioactive glass (MBG)-polycarplolactone (PCL) and extracellular matrix (ECM)-coated scaffolds in distilled water (**A**) and X-ray photoelectron spectra before and after ECM coating (**B**).

by PCL during the RP extrusion process, although the scaffolds still exhibited high bioactivity from MBG. Several sharp Ca and P peaks in the XPS spectra of the ECM-coated scaffolds were newly detected, suggesting the formation of HA on the surface of the scaffolds.[28] In addition, the detection of an N peak around 397 eV provided evidence of the presence of Col I on the surface of the ECM-coated scaffolds. Interestingly, a larger amount of collagen (5.5 ± 0.7 μg cm^{-3}) adsorbed to the MBG-PCL scaffold by the coprecipitation process of collagen and HA in SBF, compared with the scaffold coated only with single collagen in aqueous condition (3.2 ± 0.2 μg cm^{-3}) under the same conditions such as concentration of collagen and immersing time, possibly due to high interactions between HA and collagen from good protein affinity of HA (Figure 3).[37]

The wettability of the material surface is one of the key parameters affecting the adhesion and spreading of osteoblastic cells and determines subsequent processes such as cell morphology, proliferation, and differentiation.[38] Osteogenic cells tend to prefer hydrophilic surfaces rather than hydrophobic surfaces. To test the effects of ECM component coating on the wettability of scaffolds, we prepared scaffolds without pores by extruding paste in succession using RP systems (Figure S3). The water contact angle of the MBG-PCL scaffolds after applying water droplets for 60 seconds was 74.3°, whereas the water contact angle of PCL was 81.3°. The hydrophilicity of PCL improved by mixing with MBG but remained low due to limited exposure of MBG on the scaffold surface. Meanwhile, the water contact angle of the ECM-coated scaffolds was dramatically changed to 20.1°, suggesting that the hydrophilicity of the scaffolds significantly improved by coating with the ECM components (Figure 4A–C). The hydrophilic surface of the scaffolds may have been responsible for the increase in cell attachment and osteoconduction. The mechanical properties of the MBG-PCL scaffolds did not decrease during the biomimetic

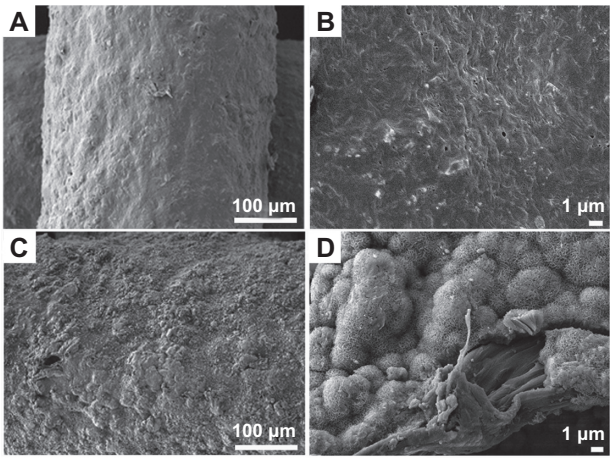

Figure 2 Field emission scanning electron microscopy images of mesoporous bioactive glass and polycarplolactone scaffolds before (**A**) and (**B**) and after (**C**) and (**D**) extracellular matrix component coating. (**B**) and (**D**) are the high magnification images of (**A**) and (**B**), respectively.

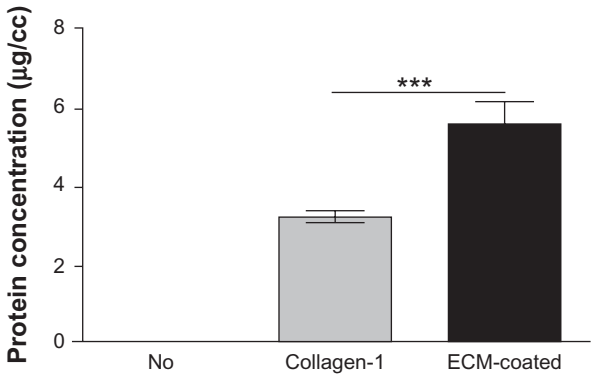

Figure 3 Comparison of the protein adsorption amount.
Note: ***$P < 0.001$.
Abbreviation: ECM, extracellular matrix.

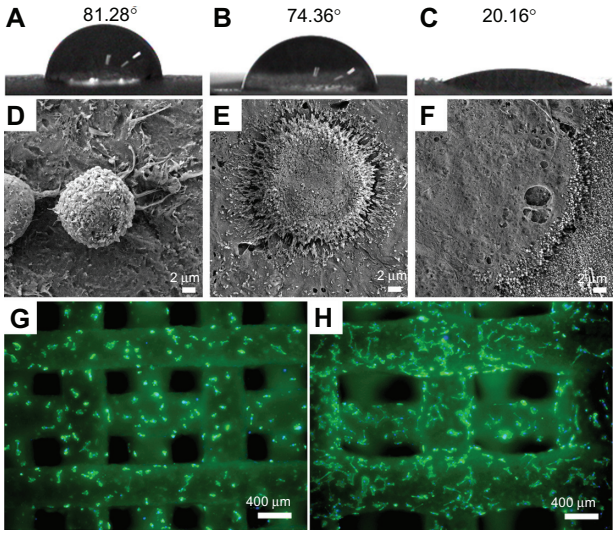

Figure 4 Wettability of polycarplolactone (PCL) (**A**) and mesoporous bioactive glass (MBG)-PCL scaffolds without (**B**) and with (**C**) extracellular matrix (ECM) component coating. (**D**-**F**) are field emission scanning electron microscopy images of initial cell attachment on PCL (**D**), MBG-PCL (**E**), and ECM-coated (**F**) scaffolds at 0.5 hours after seeding, and (**G**) and (**H**) are top view fluorescence microscope images of MBG-PCL (**G**) and ECM-coated (**H**) scaffolds after 6 hours of seeding.

coating process. The compressive moduli of the MBG-PCL and the ECM-coated scaffolds were 17.2 ± 2.4 MPa and 17.1 ± 1.9 MPa, respectively.

Effect of ECM component coating on the preosteoblast cell behavior

HA generally plays a key role in bone bonding with BG, and HA/collagen promotes the early stage of proliferation, differentiation, and bone mineralization.[27,29,39,40] The effects of coating with ECM components on cellular behavior were evaluated in vitro by studying the behavior of mouse calvaria-derived preosteoblast MC3T3-E1 cells. The spreading of cells at the initial stage is an important step for essential biological processes such as proliferation.[29] The improved hydrophilicity of the scaffolds greatly affected the enhancement of initial cell affinity. Figure 4D–F shows the adhesion and spreading morphology of MC3T3-E1 cells on the PCL-, MBG-PCL-, and ECM-coated scaffolds after 30 minutes of incubation. Cells on the PCL scaffolds were spherical in shape without spreading, whereas the appearance of cells on MBG-PCL scaffolds were more spread out with numerous filopodia and lamellipodia. Faster attachment, higher degree of cell extension, and flattened morphology with numerous filopodia and lamellipodia were observed in the cells on ECM-coated scaffolds, proving the high efficiency of ECM coating on initial cell attachment. Similar phenomena can be confirmed by fluorescent microscopic images. Figure 4G and H shows top view fluorescent microscopic images of cell growth on the MBG-PCL- and ECM-coated scaffolds after 6 hours of incubation, respectively. A higher degree of cell extension and growth was observed in the cells on ECM-coated scaffolds than MBG-PCL, proving the positive efficiency of ECM component coating on cell attachment and growth.

The initial cell attachment efficiency after 3 hours of incubation, evaluating MTT study, proved the favorable effect of ECM coating (Figure 5A). The highest rate of cellular attachment was observed in the ECM-coated scaffolds, whereas the PCL scaffolds showed the lowest rate. There was also a clear difference in the cell proliferation behaviors of scaffolds depending on their surface properties for all testing periods from 1 to 7 days of culture (Figure 5B). The ECM-coated scaffolds displayed the highest increase in the number of cells for all proliferation periods, indicating meaningful effect of the ECM components on the cell proliferation behavior.

The most notable effect of ECM coating was observed on the osteoblast differentiation behavior. The differentiation of cells cultured on PCL-, MBG-PCL-, and ECM-coated scaffolds was assessed in terms of the ALP activity of MC3T3-E1 cells at 3, 7, and 14 days as shown in Figure 5C. It is known that the ALP activity of MC3T3-E1 cells increases after differentiation and then decreases at the beginning of cell mineralization.[41] The ALP activity of the ECM-coated sample significantly increased at Day 7 and then decreased, indicating the upregulated osteoblastic differentiation of the cells at Day 7 and the start of cell mineralization at Day 14, whereas the ALP activities of both PCL and MBG-PCL scaffolds slowly increased throughout the entire tested periods. To check the effect of each ECM component on differentiated osteoblast functions, the ALP activity of MC3T3-E1 cells cultured on the MBG-PCL scaffolds coated with HA and collagen was also assessed separately for the same culturing periods (Figure 6). ALP level in HA-coated scaffolds was largely increased at Day 7, whereas the ALP level in collagen-coated scaffolds was increased at Day 14. Both coating of HA and collagen on MBG-PCL scaffolds is effective in enhancing the differentiation of cells, but HA initiates an earlier stage of differentiation than collagen. Meanwhile, the coating of both HA and collagen at the same time by our coprecipitation method using high bioactivity of MBG could promote the synergistic effect of both components and lead to a much better effect on inducing differentiation of osteoblast cells than the coating of individual components. The differences of ALP activity of MBG-PCL scaffolds with a different ECM component coating condition are mainly caused by the different effect of each component on the cell functions,

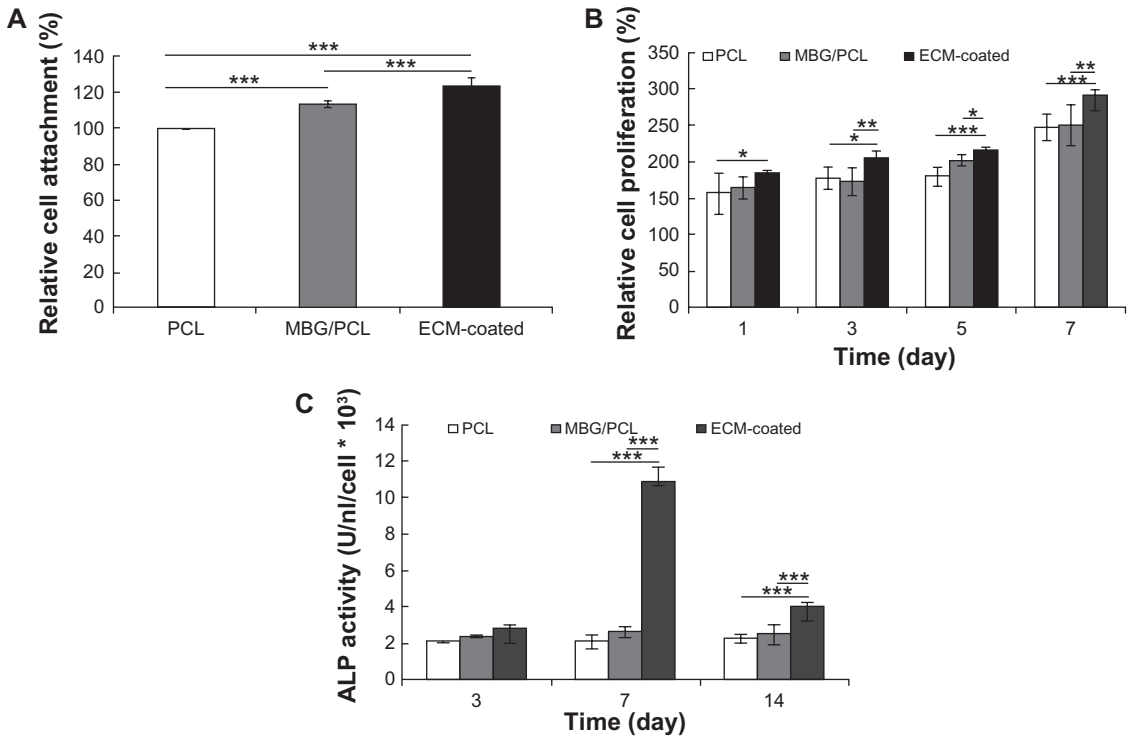

Figure 5 Initial MEC3T3-E1 cell attachment at 3 hours of culture (**A**), proliferation at 1, 3, 5, and 7 days of culture (**B**), and alkaline phosphate activity at 3, 7, and 14 days of culture (**C**) on three types of scaffolds expressed as a percentage of cell number.

Notes: Data are presented as the mean ± standard deviation (n = 5 samples per group). Differentiation from ECM-coated scaffolds (*$P < 0.05$, **$P < 0.01$, and ***$P < 0.001$).

Abbreviations: ECM, extracellular matrix; MBG, mesoporous bioactive glass; PCL, polycarplolactone.

because all scaffolds were treated using the precoating process under the same conditions, which may reduce abrupt initial pH variation.

Similar results were obtained from real-time PCR analysis at 4 and 7 days, as shown in Figure 7. Key osteoblast genes, such as RUNX2, Col I, ALP, osteopontin (OP), and osteocalcine (OC), were selected to evaluate the defect in the differentiation process at mRNA level.[42–44] RUNX2 is the master gene in osteogenesis and is the key transcription factor regulating osteoblast differentiation.[45] The expression of RUNX2 in all of the samples steadily increased over time. In particular, ECM-coated scaffolds expressed the highest level of RUNX2 from the early stage at Day 4. Col 1 is regularly used as an early marker of osteoblast differentiation. The level of Col 1 in the ECM-coated scaffolds was the highest at Day 4 but downregulated at Day 7 when differentiation started. ALP is another early-stage marker of osteoblast differentiation and function in making phosphate available for calcification. ALP was expressed at the same level in both the MBG-PCL- and ECM-coated scaffolds, whereas it was expressed much lower in the PCL scaffold at Day 4. ALP of the ECM-coated scaffolds was expressed at the highest level after 7 days. OP is a mineral-binding protein found in bone ECM. It associates with biomineralization of ECM into bone and is often used as a middle-stage marker of osteogenic differentiation. The OP level of ECM-coated scaffold was expressed the highest throughout the study and significantly increased at Day 7. OC is secreted by osteoblasts and plays a role in mineralization and calcium

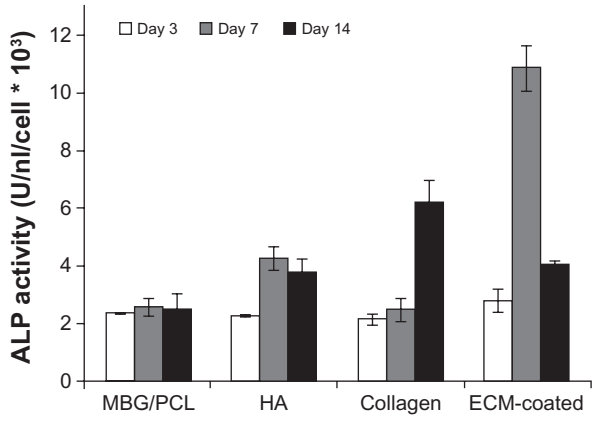

Figure 6 ALP activity of MT3T3-E1 cells on scaffolds with different surface conditions at 3, 7, and 14 days of culture.

Note: Data are presented as the mean ± standard deviation (n = 5 samples per group).

Abbreviations: ALP, alkaline phosphate; ECM, extracellular matrix; HA, hydroxy apatite; MBG, mesoporous bioactive glass; PCL, polycarplolactone.

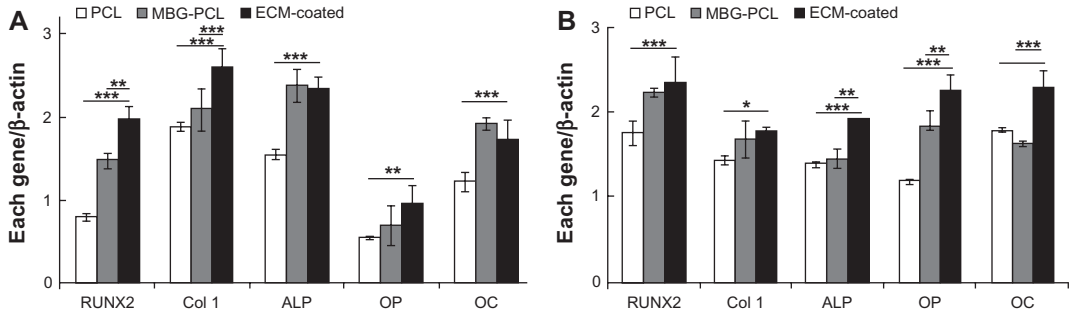

Figure 7 Quantitative real-time polymerase chain reaction analysis of RUNX2, collagen-I, ALP, OP, and OC mRNA expression in cells grown on each scaffold at 4 (**A**) and 7 (**B**) days of culture.

Note: Data are presented as the mean ± standard deviation (at least n = 3 samples per group). Differentiation from ECM-coated scaffolds (*$P < 0.05$, **$P < 0.01$, and ***$P < 0.001$).

Abbreviations: ALP, alkaline phosphate; ECM, extracellular matrix; MBG, mesoporous bioactive glass; OC, osteocalcine; OP, osteopontin; PCL, polycarplolactone.

ion homeostasis. Consequently, it is often used as a terminal marker of osteoblast differentiation. The highest level of OC was observed in ECM-coated scaffolds at Day 7. The early increased expression of OP and OC in cells grown on ECM-coated scaffolds may be due to the fact that mineralization occurred much sooner. That is, the presence of ECM components may have been the key factor promoting stimulation of the osteogenic differentiation of osteoblast cells. These results also show that our suggested coating process on MBG/PCL scaffolds was effective in enhancing the applicability of MBG/PCL scaffolds to bone tissue regeneration.

The advantage of using an RP technique to produce 3D scaffolds is the construction of a highly porous and well-interconnected 3D structure.[46,47] These structural properties allow efficient cell migration, vascularization, and tissue in-growth. The 3D cell movement is essential for 3D tissue in-growth through 3D scaffolds. Meanwhile, the surface properties of 3D scaffolds are also important for promoting sufficient tissue regeneration. The ECM-coated scaffolds display good cell affinity and consequently promote good cell migration as well as penetration within the interior of the 3D scaffolds. Figure 8 shows top view FE-SEM images of cells on the ECM-coated scaffolds after 5 days of incubation. The morphology and distribution of the cells on each strut were similar from the first layer (Figure 8A) to the fourth layer (Figure 8D), indicating good cell penetration into ECM-coated scaffolds. Figure 9 shows FE-SEM images of the PCL-, MBG-PCL-, and ECM-coated scaffolds before and after 21 days of cell culture. Although all three scaffolds had the same structure, their cell growth progressed differently. Less tissue sheet formation was observed on the PCL scaffold, especially within the interface of each strut (Figure 9A). The MBG-PCL scaffold showed the formation of denser cell sheets compared with the PCL, and therefore better function as a bone scaffold (Figure 9B). In contrast, there was greater dense cell and tissue sheet formation on the ECM-coated scaffolds, revealing a significant role for ECM components in tissue distribution (Figure 9C). These results suggest that the biomimetic ECM component coating process on MBG/PCL scaffold using a high bioactivity of MBG is effective for enhancing proliferation, osteogenic differentiation, penetration, and growth of cells, and provides high potential possibilities of MBG/PCL scaffolds in the field of bone tissue regeneration.

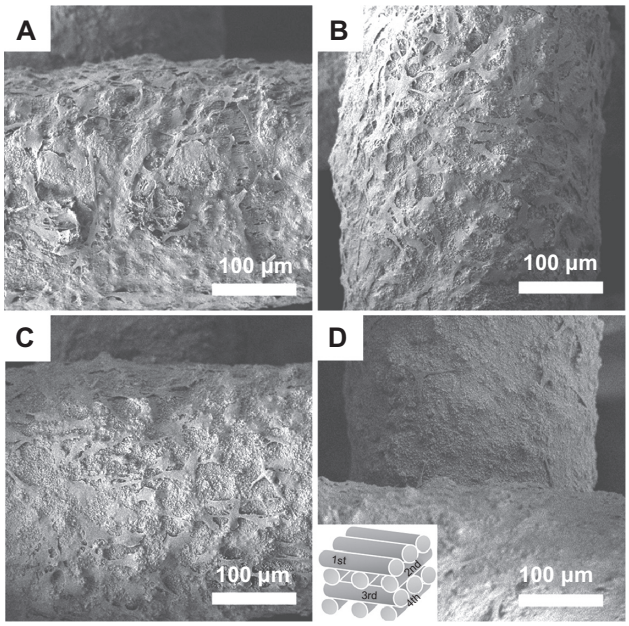

Figure 8 Field emission scanning electron microscopy images of extracellular matrix-coated scaffolds after 5 days of culture of MC3T3-E1 cell: first (**A**), second (**B**), third (**C**), and fourth layer (**D**).

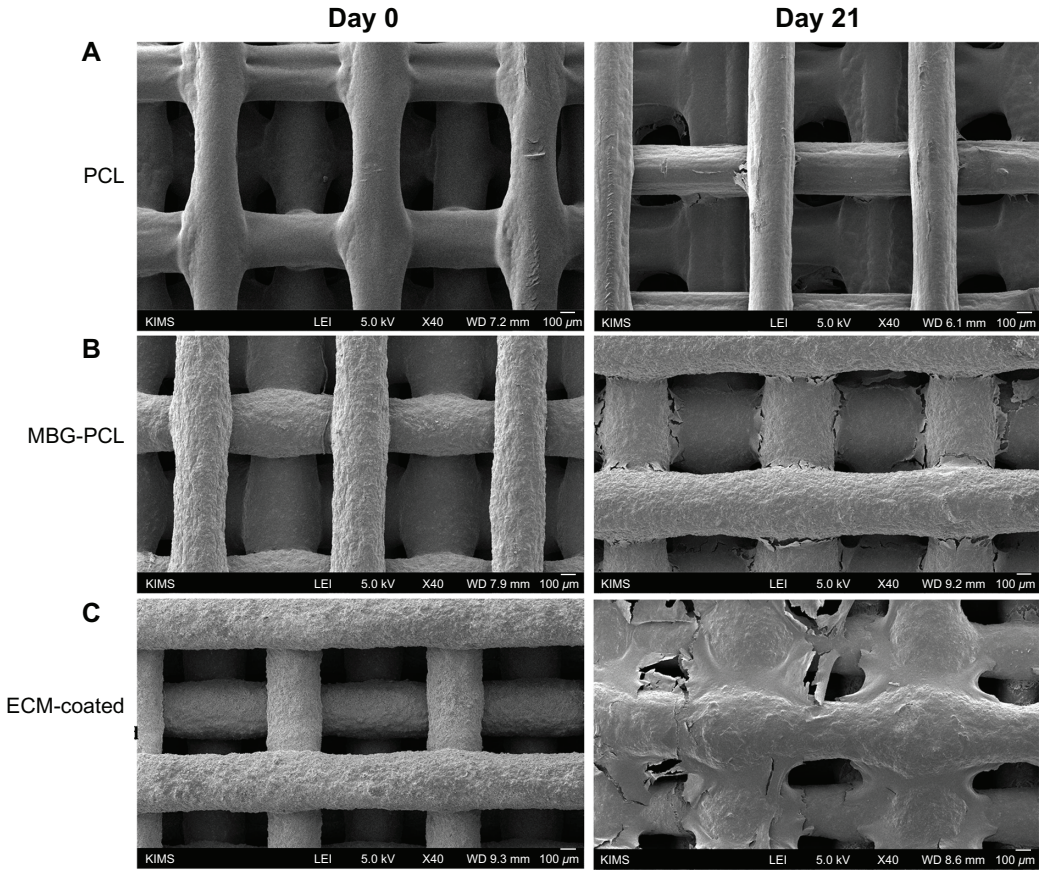

Figure 9 Field emission scanning electron microscopy images of cell growth before (left) and after 21 days (right) of culture of MC3T2-E1 cells on polycarplolactone (PCL), mesoporous bioactive glass (MBG)-PCL, and extracellular matrix (ECM)-coated scaffolds.

Conclusion

A scaffold must meet several specific requirements to achieve the goal of bone reconstruction. Ideal scaffolds should have several features, including high porosity with 3D interconnected pore structures, bioactivity, biodegradability, biocompatibility, osteoconductivity, and sufficient mechanical properties. Our proposed scaffolds ideally satisfied these conditions. That is, the RP technique provided an easily controllable and highly interconnected 3D pore structure with 70% porosity. MBG supplied high bioactivity, and both MBG and PCL were found to be biodegradable and biocompatible. The combination of MBG and PCL may have provided enhanced mechanical properties compared with the case of using each material alone. ECM component coating using high bioactivity of MBG on the MBG-PCL scaffolds promoted high osteoconductivity. This biomimetic coating process was also helpful in preventing negative effects of local pH variations during the initial ion-leaching. The mesoporosity of MBG should also make possible the controlled release of drugs into scaffolds. We hope that this simple and reproducible process can be adapted for the preparation of various scaffolds for use in tissue regeneration. More detailed studies in vivo are currently in progress.

Acknowledgment

This work was supported by the Mid-career Researcher Program through a National Research Foundation of Korea grant funded by the Korean Ministry of Education, Science and Technology (No. 2011-0017572).

Disclosure

The authors report no conflicts of interest in this work.

References

1. Wan Y, Zhao D. On the controllable soft-templating approach to mesoporous silicate. *Chem Rev*. 2007;107:2821–2860.
2. Hartmann H. Ordered mesoporous materials for bioadsorption and biocatalysis. *Chem Mater*. 2005;17:4577–4593.
3. Colilla M, Manzano M, Vallet-Regí M. Recent advances in ceramic implants as drug delivery systems for biomedical application. *Int J Nanomedicine*. 2008;3:403–414.
4. Lee CH, Lin TS, Mou CY. Mesoporous materials for encapsulating enzymes. *Nano Today*. 2009;4:165–179.

5. Vallet-Regí M, Ruiz-González L, Izquierdo-Barba I, González-Calbet JM. Revisiting silica based ordered mesoporous materials: medical applications. *J Mater Chem*. 2006;16:26–31.
6. Yan X, Yu C, Zhou X, Tang J, Zhao D. Highly ordered mesoporous bioactive glasses with superior in vitro bone-forming bioactivities. *Angew Chem Int Ed Engl*. 2004;43:5980–5984.
7. López-Niriega A, Arcos D, Izquiedo-Barba I, Sakamoto Y, Terasaki O, Vallet-Regi M. Ordered mesoporous bioactive glasses for bone tissue regeneration. *Chem Mater*. 2006;18:3137–3144.
8. Shi QH, Wang JF, Zhang JP, Fan J, Stucky GD. Rapid-setting mesoporous bioactive glass cements that induce accelerated in vitro apatite formation. *Adv Mater*. 2006;18:1038–1042.
9. Ostomel TA, Shi Q, Tsung CK, Liang H, Stucky GD. Spherical bioactive glass with enhanced rates of hydroxyapatite deposition and hemostatic activity. *Small*. 2006;11:1261–1265.
10. Yun HS, Kim SE, Hyeon YT. Design and preparation of bioactive glasses with hierarchical pore networks. *Chem Commun (Camb)*. 2007: 2139–2141.
11. Yun HS, Kim SE, Hyun YT, Heo SJ, Shin JW. Three-dimensional mesoporous-giantporous inorganic/organic composite scaffolds for tissue engineering. *Chem Mater*. 2007;19:6363–6366.
12. Li X, Wang X, Chen H, Jiang P, Dong X, Shi J. Hierarchically porous bioactive glass scaffolds synthesized with a PUF and P123 cotemplated approach. *Chem Mater*. 2007;19:4322–4326.
13. Zhu Y, Wu C, Ramaswamy Y, et al. Preparation, characterization and in vitro bioactivity of mesoporous bioactive glasses (MBGs) scaffolds for bone tissue engineering. *Micropor Mesopor Mater*. 2008;112: 494–503.
14. Zhu Y, Kaskel S. Comparision of the in vitro bioactivity and drug release property of mesoporous bioactive glasses (MBGs) and bioactive glasses (BGs) scaffolds. *Micropor Mesopor Mater*. 2009;118:176–182.
15. Yun HS, Kim SE, Hyun YT. Preparation of bioactive glass ceramic beads with hierarchical pore structure using polymer self-assembly technique. *Mater Chem Phys*. 2009;115:670–676.
16. Peña J, Román J, Cabanas MV, Vallet-Regí M. An alternative technique to shape scaffolds with hierarchical porosity at physiological temperature. *Acta Biomater*. 2010;6:1288–1296.
17. Wu C, Zhang Y, Zhu Y, Friis T, Xiao Y. Structure-property relationships of silk-modified mesoporous bioglass scaffolds. *Biomaterials*. 2010;31:3429–3438.
18. Alcaide M, Portolés P, López-Noriega A, Arcos D, Vallet-Regí M, Portolés MT. Interaction of an ordered mesoporous bioactive glass with osteoblasts, fibroblasts and lymphocytes, demonstrating its biocompatibility as a potential bone graft material. *Acta Biomater*. 2010;6: 892–899.
19. Yun HS, Kim SH, Lee S, Song IH. Synthesis of high surface area mesoporous bioactive glass nanospheres. *Mater Lett*. 2010;64:1850–1853.
20. Yun HS, Kim SE, Park EK. Bioactive glass-poly (ε-caprolactone) composite scaffolds with 3 dimensionally hierarchical pore networks. *Mater Sci Eng C*. 2011;31:198–205.
21. Wu C, Luo Y, Cuniberti G, Xiao Y, Gelinsky M. Three-dimensional printing of hierarchical and tough mesoporous bioactive glass scaffolds with controllable pore architecture, excellent mechanical strength and mineralization ability. *Acta Biomater*. 2011;7:2644–2650.
22. Hutmacher DW. Scaffolds in tissue engineering bone and cartilage. *Biomaterials*. 2000;21:2529–2543.
23. Karageorgiou V, Kaplan D. Porosity of 3D biomaterial scaffolds and osteogenesis. *Biomaterials*. 2005;26:5474–5491.
24. Stevens MM. Biomaterials for bone tissue engineering. *Mater Today*. 2008;11:18–25.
25. Hollister SJ. Scaffold design and manufacturing: from concept to clinic. *Adv Mater*. 2009;21:3330–3342.
26. Yun HS, Park JW, Kim SH, Kim YJ, Jang JH. Effect of the pore structure of bioactive glass balls on biocompatibility in vitro and in vivo. *Acta Biomater*. 2011;7:2651–2660.
27. Chen Y, Mak AF, Wang M, Li JS, Wong MS. In vitro behavior of osteoblast-like cells on PLLA films with a biomimetic apatite or apatite/collagen composite coating. *J Mater Sci Mater Med*. 2008;19: 2261–2268.
28. Arafat MT, Lam CXF, Ekaputra AK, Wong SY, Li X, Gibson I. Biomimetic composite coating on rapid prototyped scaffolds for bone tissue engineering. *Acta Biomater*. 2011;7:809–820.
29. Olmo N, Martín AI, Salinas AJ, Turnay J, Vallet-Regí M, Lizarbe MA. Bioactive sol-gel glasses with and without a hydroxycarbonate apatite layer as substrates for osteoblast cell adhesion and proliferation. *Biomaterials*. 2003;24:3383–3393.
30. Lynch MP, Stein JL, Stein GS, Lian JB. The influence of type I collagen on the development and maintenance of the osteoblast phenotype in primary and passaged rat calvarial osteoblasts: modification of expression of genes supporting cell growth, adhesion, and extracellular matrix mineralization. *Exp Cell Res*. 1995;216:35–45.
31. Boyan BD, Hummert TW, Dean DD, Schwartz Z. Role of material surfaces in regulating bone and cartilage cell response. *Biomaterials*. 1996;17:137–146.
32. Yun HS, Kim SE, Hyun YT. Preparation of highly cubic ordered mesoporous bioactive glasses. *Solid State Sci*. 2008;10:1083–1092.
33. Kokubo T, Takadama H. How useful is SBF in predicting in vivo bone bioactivity? *Biomaterials*. 2007;27:2907–2915.
34. Greenlee Jr, Beckham TK, Crebo AR, Malmorg JC. Glass ceramic bone implant. A light microscopic study. *J Biomed Mater Res*. 1971;6: 235–244.
35. Vitale-Brovarone C, Verné E, Robiglio L, et al. Development of glass-ceramic scaffolds for bone tissue engineering: characterization, proliferation of human osteoblasts and nodule formation. *Acta Biomater*. 2007;3:199–208.
36. Loty C, Sautier JM, Oboeuf M, et al. Bioactive glass simulates in vitro osteoblast differentiation and creates a favorable template for bone tissue formation. *J Bone Miner Res*. 2001;16:231–239.
37. Hench LL, Polak JM. Third-generation biomedical materials. *Science*. 2002;295:1014–1017.
38. Padial-Molina M, Galindo-Moreno P, Fernández-Barbero JE, et al. Role of wettability and nanoroughness on interactions between osteoblast and modified silicon surfaces. *Acta Biomater*. 2011;7:771–778.
39. Wahl DA, Czernuszka JT. Collagen-hydroxyapatite composites for hard tissue repair. *Eur Cell Mater*. 2006;11:43–56.
40. Li J, Chen Y, Mak AF, Tuan RS, Li L, Li Y. A one-step method to fabricate PLLA scaffolds with deposition of bioactive hydroxyapatite and collagen using ice-based macroporogens. *Acta Biomater*. 2010;6: 2013–2019.
41. Kuboki Y, Kudo A, Mizuno M, Kawamura M. Time-dependent changes of collagen cross-links and their precursors in the culture of osteogenic cells. *Calcif Tissue Int*. 1992;50:473–480.
42. Jell G, Stevens MM. Gene activation by bioactive glasses. *J Mater Sci Mater Med*. 2006;17:997–1002.
43. Setzer B, Bächle M, Metzger MC, Kohal RJ. The gene-expression and phenotypic response of hFOB 1.19 osteoblasts to surface-modified titanium and zirconia. *Biomaterials*. 2009;30:979–990.
44. Stangenberg L, Schaefer DJ, Buettner O, et al. Differentiation of osteoblasts in three-dimensional culture in processed cancellous bone matrix: quantitative analysis of gene expression based on real-time reverse transcription-polymerase chain reaction. *Tissue Eng*. 2005;11: 855–864.
45. Komori T. Regulation of bone development and extracellular matrix genes by RUNX2. *Cell Tissue Res*. 2010;339:189–195.
46. Hollister SJ. Porous scaffold design for tissue engineering. *Nat Mater*. 2005;4:518–524.
47. Landers R, Hübner U, Schmelzeisen R, Mülhaupt R. Rapid prototyping of scaffolds derived from thermoreversible hydrogels and tailored for applications in tissue engineering. *Biomaterials*. 2003;23: 4437–4447.

Supplementary figures

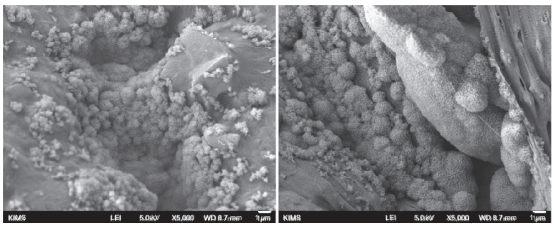

Figure S1 Field emission scanning electron microscopy images of mesoporous bioactive glass and polycarplolactone scaffold surface after immersing in simulated body fluid collagen solution for 4 hours (left) and 24 hours (right).

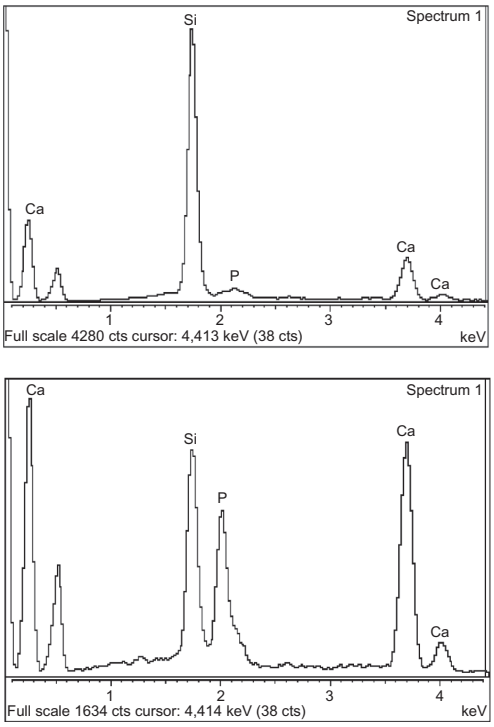

Figure S2 Electrodiagnostic studies corresponding to the surface of mesoporous bioactive glass and polycarplolactone scaffolds before (top) and after (bottom) extracellular matrix component coating.

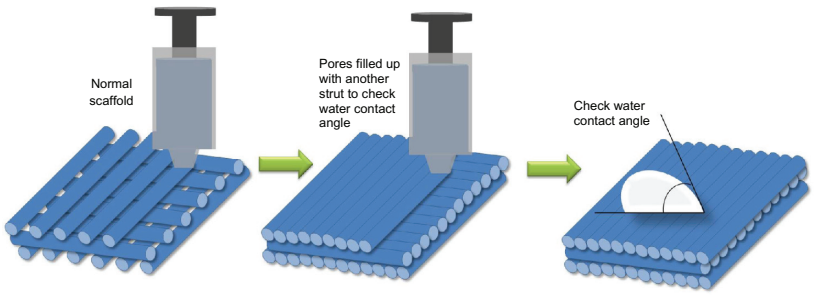

Figure S3 Sample preparation method for testing water contact angle.

International Journal of Nanomedicine

Dovepress

Publish your work in this journal

The International Journal of Nanomedicine is an international, peer-reviewed journal focusing on the application of nanotechnology in diagnostics, therapeutics, and drug delivery systems throughout the biomedical field. This journal is indexed on PubMed Central, MedLine, CAS, SciSearch®, Current Contents®/Clinical Medicine, Journal Citation Reports/Science Edition, EMBase, Scopus and the Elsevier Bibliographic databases. The manuscript management system is completely online and includes a very quick and fair peer-review system, which is all easy to use. Visit http://www.dovepress.com/testimonials.php to read real quotes from published authors.

Submit your manuscript here: http://www.dovepress.com/international-journal-of-nanomedicine-journal